

12-5-2016

## Interface magnetization transition via minority spin injection

F. Fang

*William & Mary*, luepke@wm.edu

H. Zhai

*William & Mary*

X. Ma

*William & Mary*

Y. W. Yin

Qi Li

*See next page for additional authors*

Follow this and additional works at: <https://scholarworks.wm.edu/aspubs>

---

### Recommended Citation

Fang, F.; Zhai, H.; Ma, X.; Yin, Y. W.; Li, Qi; and Lupke, G., Interface magnetization transition via minority spin injection (2016). *APPLIED PHYSICS LETTERS*, 109(23).  
10.1063/1.4972035

This Article is brought to you for free and open access by the Arts and Sciences at W&M ScholarWorks. It has been accepted for inclusion in Arts & Sciences Articles by an authorized administrator of W&M ScholarWorks. For more information, please contact [scholarworks@wm.edu](mailto:scholarworks@wm.edu).

---

**Authors**

F. Fang, H. Zhai, X. Ma, Y. W. Yin, Qi Li, and G. Lupke

## Interface magnetization transition via minority spin injection

F. Fang,<sup>1</sup> H. Zhai,<sup>1</sup> X. Ma,<sup>1</sup> Y. W. Yin,<sup>2</sup> Qi Li,<sup>2</sup> and G. Lüpke<sup>1,a)</sup>

<sup>1</sup>Department of Applied Science, College of William and Mary, Williamsburg, Virginia 23187, USA

<sup>2</sup>Department of Physics, Pennsylvania State University, University Park, Pennsylvania 16802, USA

(Received 12 July 2016; accepted 29 November 2016; published online 7 December 2016)

The interface magnetization of n-type BaTiO<sub>3</sub>/La<sub>0.7</sub>Sr<sub>0.3</sub>MnO<sub>3</sub> heterojunction is selectively probed by magnetic second-harmonic generation at 80 K. The injection of minority spins at the interface causes a sudden, reversible transition of the spin alignment of interfacial Mn ions from ferromagnetic to antiferromagnetic exchange coupled, while the bulk magnetization remains unchanged. We attribute the emergent interfacial antiferromagnetic interactions to weakening of the double-exchange mechanism caused by the strong Hund's rule coupling between injected minority spins and local magnetic moments. The effect is robust and may serve as a viable route for electronic and spintronic applications. *Published by AIP Publishing.* [<http://dx.doi.org/10.1063/1.4972035>]

Engineered thin-film heterostructures designed for the electric control of magnetic properties, the so-called *magneto-electric (ME) interfaces*, present a unique route towards using the spin degree of freedom in electronic devices.<sup>1–15</sup> Recently, researchers employed polarized ferroelectric (FE) layers, e.g., Pb(Zr<sub>0.2</sub>Ti<sub>0.8</sub>)O<sub>3</sub> (PZT) or BaTiO<sub>3</sub> (BTO), to alter the magnetic state at the interface of the ferromagnetic (FM) layer, such as La<sub>0.7</sub>Sr<sub>0.3</sub>MnO<sub>3</sub> (LSMO)<sup>16,17</sup> and CoFe<sub>2</sub>O<sub>4</sub>.<sup>18</sup> Moreover, Yin *et al.* observed a giant tunneling electroresistance ratio of ~3300% by inserting an ultrathin La<sub>0.5</sub>Ca<sub>0.5</sub>MnO<sub>3</sub> (LCMO) barrier in the junction of LSMO/BTO/LSMO.<sup>19</sup> The results suggest a ferroelectrically induced metal-insulator phase transition in the LCMO layer that is of ME origin. This has been investigated by Yi *et al.*,<sup>20</sup> who observed direct evidence for a magnetic phase transition in LCMO controlled by the FE polarization of BiFeO<sub>3</sub>. The interfacial ME coupling effect is mainly derived from the superexchange between Mn and Fe t<sub>2g</sub> spins.<sup>20</sup> The authors also suggest that there may be similar pathways to implement a reversible switch between ferromagnetic (FM) and antiferromagnetic (AFM) states.<sup>20</sup> In this study, we discover a unique interface ME effect that alters the interface magnetization in n-type BTO/LSMO heterojunction via the injection of minority spins.

Here, we use magnetization-induced second-harmonic generation (MSHG) to selectively probe the interface magnetization of the n-type BTO/LSMO heterojunction as a function of gate voltage  $U_g$  (Fig. 1(a)). We fabricated the indium-tin-oxide ITO (50 nm)/BTO (200 nm)/LSMO (50 nm) heterostructures epitaxially grown on SrTiO<sub>3</sub> (STO) (100) substrates by pulsed laser deposition (see [supplementary material](#)). The ITO and LSMO layer serve as top and bottom electrodes, respectively (Fig. 1(a)). Since the samples are cooled down to room temperature in a reduced oxygen atmosphere, the sufficient native oxygen vacancies in BTO are double shallow donors and will make it n-type (~10<sup>18</sup>/cm<sup>3</sup>).<sup>21</sup> The MSHG technique is well suited for probing the interfacial magnetic state where both space-inversion and time-reversal symmetries are broken.<sup>17,22,23</sup> For comparison, the magneto-optical Kerr effect (MOKE) measurements are employed to detect

the bulk magnetization (see [supplementary material](#)). All measurements are performed at 80 K. In the following, we discuss the change of magnetization as a function of  $U_g$  in terms of the magnetic contrast of the hysteresis loop (Fig. 1(b)). The magnetic contrast for a hysteresis loop is defined as<sup>17</sup>

$$A = \frac{I(+M) - I(-M)}{I(+M) + I(-M)}, \quad (1)$$

where  $I(+M)$  and  $I(-M)$  are the intensities for the two magnetization states. The magnetic contrast  $A$  can be understood as the height of the jump in the hysteresis loop divided by the sum of the intensities of both magnetizations. Figure 1(c) displays the magnetic contrast  $A$  obtained from the MSHG hysteresis loops as a function of  $U_g$  (see [supplementary material](#)). For  $U_g < U_c$  (+1 V), the interfacial LSMO is in the FM state since the magnetic contrast is obvious. Above  $U_c$ , the magnetic contrast  $A$  suddenly vanishes, indicating a magnetic transition to AFM phase since a paramagnetic phase is unlikely to occur in LSMO at 80 K due to the strong superexchange interaction of t<sub>2g</sub> electrons of neighboring Mn ions. We attribute this sudden, reversible FM-to-AFM phase transition to an interface ME effect. In contrast, the magnetic contrast  $A$  obtained from the MOKE hysteresis loops remains constant (see [supplementary material](#)), indicating that the magnetization of the LSMO bulk does not change as a function of  $U_g$  (Fig. 1(d)).

The P-V curve (Fig. 1(f)) suggests that the observed interface magnetic transition is not caused by polarization switching of the BTO layer. There is no sudden jump in the P-V curve, nor does the magnetic contrast  $A$  exhibit a hysteresis loop (Fig. 1(c)). The observed interface ME effect is therefore not related to the polarization-induced interface magnetic transition of LSMO, as observed for PZT/LSMO interface.<sup>16,17</sup> One possible explanation is that the ferroelectricity is weakened exponentially with size (for more details, see [supplementary material](#)).

Further evidence for the ME coupling mechanism is provided from the dopant dependent studies of the BTO layer. A BTO (200 nm)/LSMO (50 nm) heterojunction is prepared under the oxygen-rich conditions. The C-V measurements (see [supplementary material](#)) reveal that the oxygen-rich

<sup>a)</sup>luepke@wm.edu

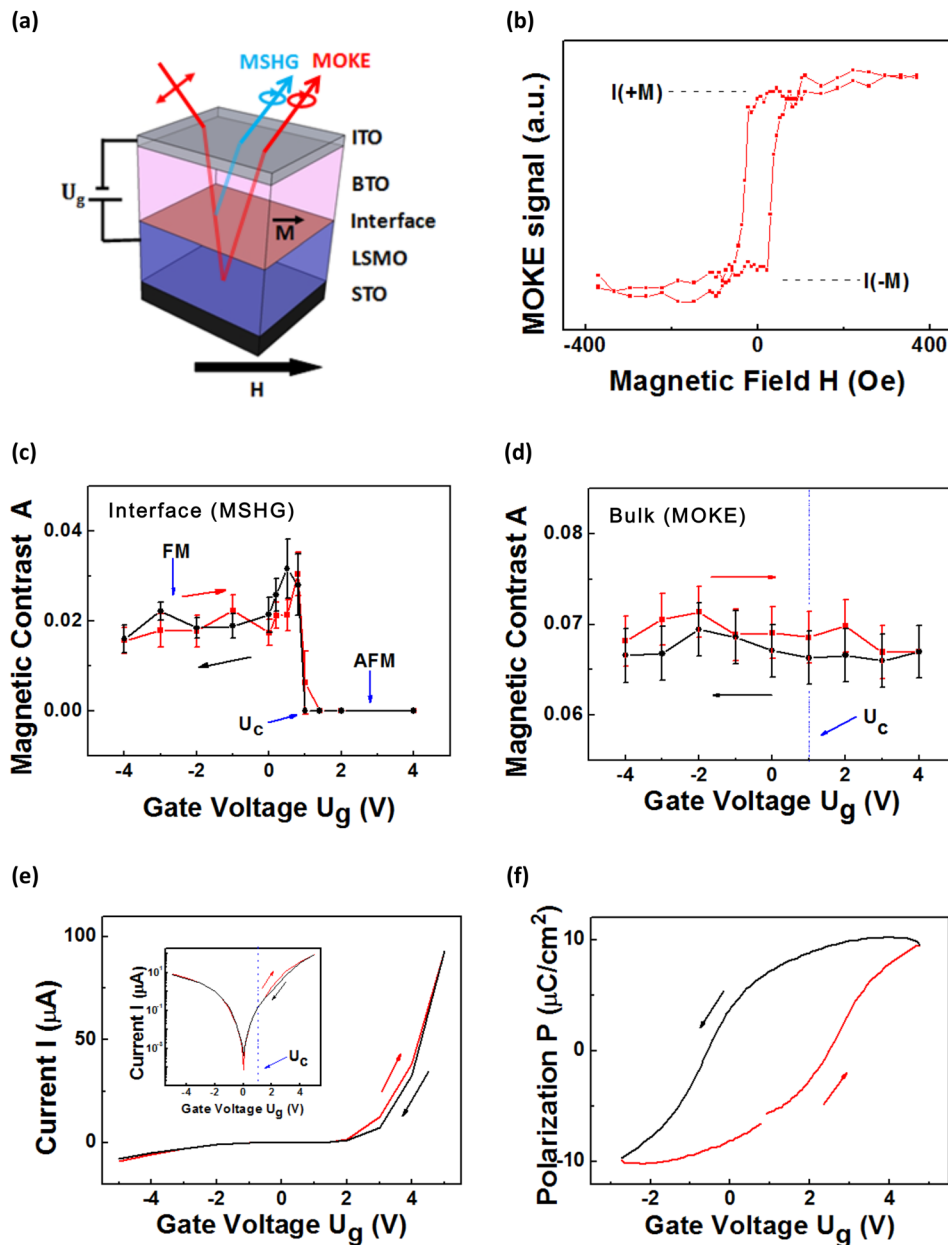


FIG. 1. (a) Schematic of the optical measurements. MOKE measures the bulk magnetization of the LSMO film, while MSHG selectively probes the interface magnetization only. (b) MOKE hysteresis loop indicating I(-M) and I(+M) used to determine the magnetic contrast  $A$  using Eq. (1). Magnetic contrast  $A$  determined from (c) MSHG and (d) MOKE measurements as a function of gate voltage  $U_g$ . The BTO/LSMO interface exhibits an FM-to-AFM phase transition at  $U_c$ , while the bulk LSMO maintains the FM state. (e) I-V curve and (f) P-V curve. Decreasing (increasing) gate voltages are labeled in black (red). All the measurements are performed at 80 K.

sample has a lower electron concentration of  $\sim 10^{17} \text{ cm}^{-3}$ , as compared to the oxygen-poor sample ( $10^{18} \text{ cm}^{-3}$ ). Figure 2(a) displays the magnetic contrast  $A$  obtained from the MSHG hysteresis loops as a function of  $U_g$  (see [supplementary material](#)). The data in Fig. 2(a) show that the magnetic transition is remarkably sharp, since the magnetic contrast (magnetization  $M$ ) approaches zero at the critical voltage  $U_c$  with infinite slope. The interface magnetic transition is shifted to a much higher critical voltage  $U_c = +6 \text{ V}$ .

We note that the P-V curve of the oxygen-rich sample (Fig. 2(b)) is comparable to the oxygen-poor sample (Fig. 1(f)), indicating further that the magnetic transition is not driven by the FE polarization. In fact,  $U_c = +6 \text{ V}$  is above the switching voltage for the FE polarization of BTO that excludes the influence from the ferroelectric properties. In contrast, the I-V characteristic of the oxygen-rich sample (Fig. 2(c)) exhibits much more rectifying behavior than the oxygen-poor sample (Fig. 1(e)). We attribute this to the lower electron (oxygen vacancy) concentration of the oxygen-rich sample.

Next, we discuss the microscopic mechanism of this unique interface ME effect. Figure 3 shows a schematic of the proposed band alignment at the n-type BTO/LSMO Schottky junction with the positive gate voltage. The band alignment of BTO/LSMO is based on the electron affinity of BTO ( $3.9 \text{ eV}$ )<sup>24</sup> and metal work function of LSMO ( $4.8 \text{ eV}$ ),<sup>25</sup> which makes the bands bend up at the interface. For FE polarization ( $P$ ) pointing away from the LSMO layer, the hole accumulation biases the interfacial LSMO layer towards the AFM insulating phase. The  $\text{La}_{0.7}\text{Sr}_{0.3}\text{MnO}_3$ , however, has stoichiometry that is far enough from the phase boundary, and a change in magnetic order is not expected owing solely to a build-up of screening charge.<sup>19</sup> At the reverse gate voltage  $U_g$ , no spin injection current occurs at the n-type BTO/LSMO interface. The nearby majority spins of  $\text{Mn}^{3+}$  and  $\text{Mn}^{4+}$  ions are double-exchange coupled, leading to a ferromagnetic state, as depicted in Fig. 4(a).

On the other hand, for a positive gate voltage applied to the LSMO layer, an electron current ( $J^-$ ) begins to flow

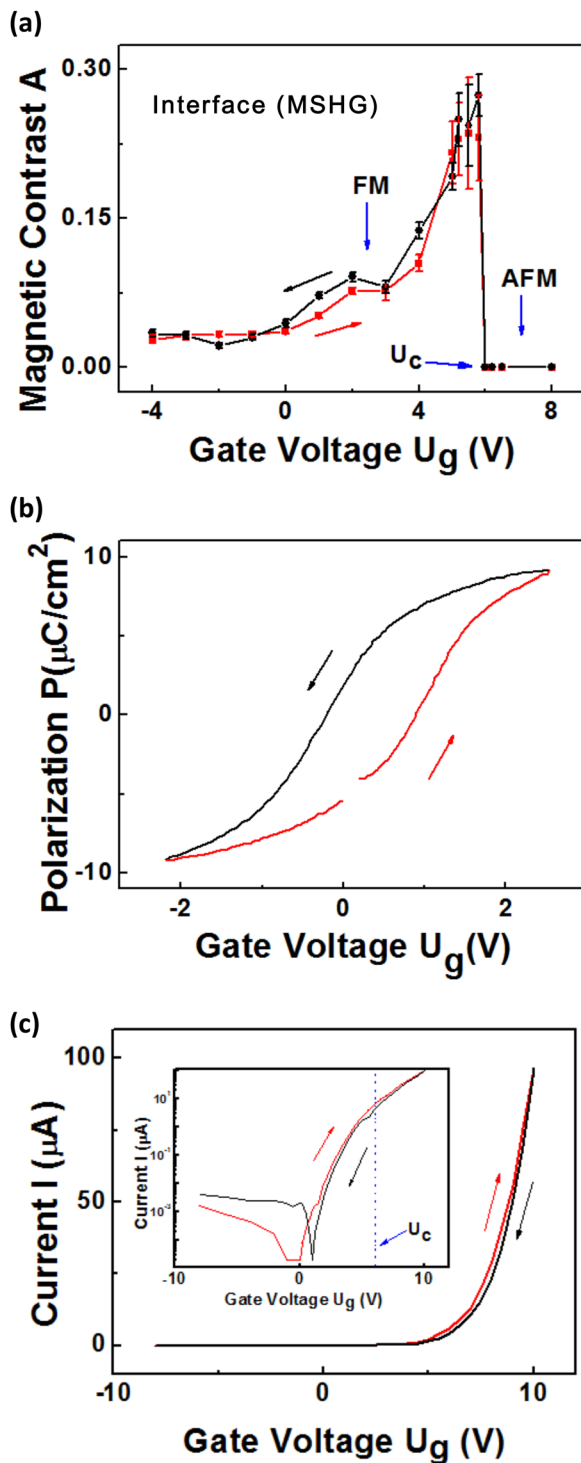


FIG. 2. (a) Magnetic contrast  $A$  determined from MSHG hysteresis loops as a function of gate voltage  $U_g$ . The oxygen-rich BTO/LSMO heterojunction exhibits an interface magnetic transition at  $U_c = +6$  V, which is much higher than for the oxygen-poor sample (Fig. 1). (b) P-V curve and (c) I-V curve. Decreasing (increasing) gate voltages are labeled in black (red). All the measurements are performed at 80 K.

across the BTO/LSMO heterojunction (Fig. 1(e)). Both the spin-up and spin-down electrons will be injected from the conduction band of BTO into the interfacial LSMO layer, since the spin polarization of LSMO surfaces extracted from the transport measurements usually yield less than 95%.<sup>26</sup> The majority spin-up electrons will quickly relax to the Fermi level and conduct through the LSMO layer (Fig. 3). In

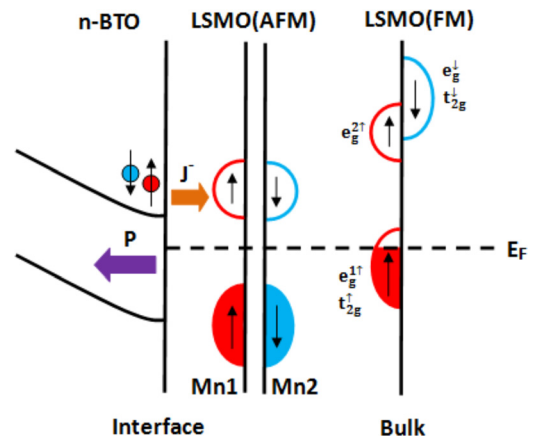


FIG. 3. Schematic band diagram of the n-type BTO/LSMO Schottky junction for  $U_g > U_c$ , depicting the electron current  $J$ , ferroelectric polarization  $P$ , and considering an AFM-ordered LSMO interface layer and a half-metallic LSMO electrode with only spin-up states at the Fermi level  $E_F$ .

contrast, the minority spin-down electrons will accumulate at the interface, since the spin-hopping process  $t$  is blocked by the strong interaction with the local spins due to the large Hund's rule coupling  $J_H$  (Fig. 4(b)). This will weaken the double-exchange mechanism and hence reduce the ferromagnetic coupling between the Mn ions at the LSMO interface. At a critical gate voltage  $U_c$ , the injected minority spin-down electrons will reduce the double-exchange mechanism such that the AFM super-exchange interaction will dominate, and the interfacial LSMO layer will undergo an FM-to-AFM phase transition. This magnetic reconstruction will occur in the first Mn layer at the interface, since the minority spin-down electrons will strongly scatter with electrons, phonons and magnons, resulting in the fast spin-flip processes.<sup>27</sup> The primary one is the Elliott-Yafet-type spin-flip scattering, which usually takes place on a time scale of a few hundred femtoseconds.<sup>28</sup> For comparison, the characteristic time-scales of double- and super-exchange coupling,  $J \approx -10$  K and 7 K,<sup>29</sup> can be estimated via the Heisenberg relation  $\tau = \hbar/|J| \approx 4$  ps. Hence, the magnetic reconstruction will occur predominantly at the interface. This will also lead to spin frustration, with the competition between AFM coupling at the interface and FM ground state of bulk LSMO. To achieve a more energetically favorable state, the spins in the interfacial layer will cant along the spin direction of the bulk LSMO.

The observed interfacial magnetoelectric coupling mechanism is conceptually different from those known previously, such as FE polarization-induced changes in the lattice strain or nature of chemical bonding, and/or charge (carrier) modulation at the multiferroic heterojunction.<sup>15</sup> Both can affect the FM moments at the interface of LSMO layer, as expected from their critical phase-competitive nature in magnetism. Here, the injected minority spins through the strong Hund's interaction with the local magnetic moments causing a sudden and reversible magnetic transition at the LSMO interface. The results are important for the transport properties of magnetic tunneling junctions because an interfacial magnetic transition may notably change the spin polarization of the tunneling current and thus be decisive for tunneling magnetoresistance.

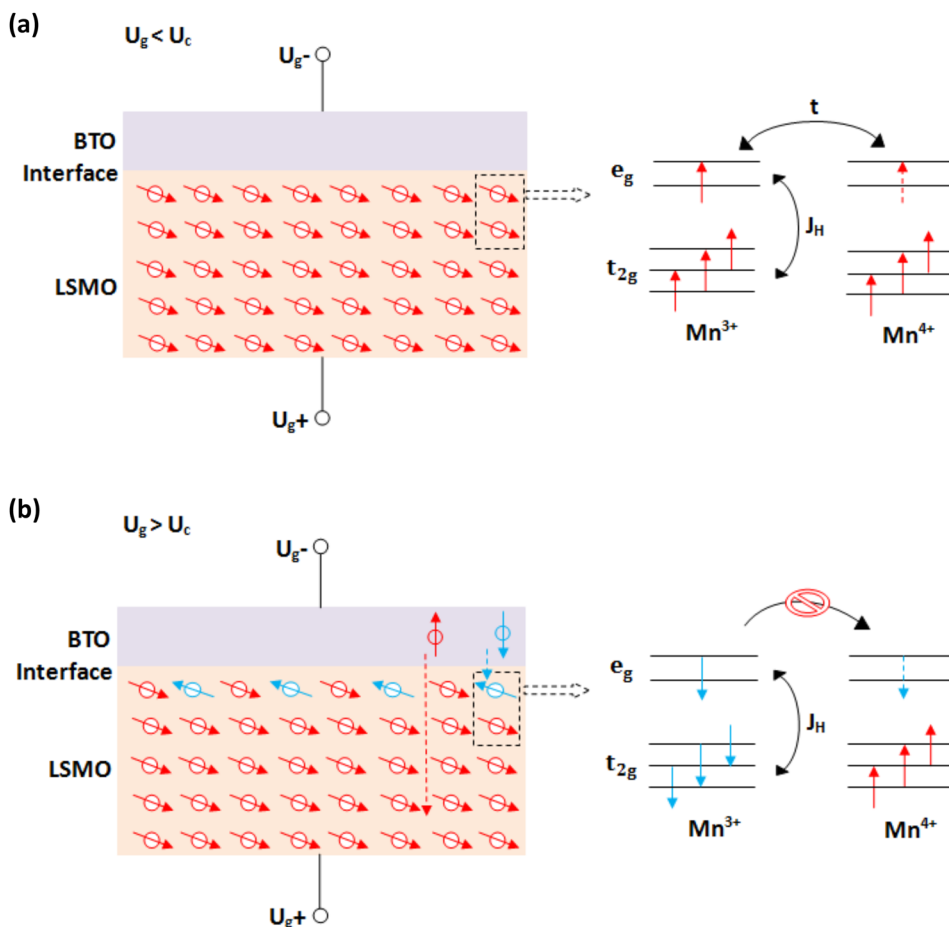


FIG. 4. (a) Below critical gate voltage  $U_c$ , majority spins (red arrows) of  $\text{Mn}^{3+}$  and  $\text{Mn}^{4+}$  ions are double-exchange coupled (right panel), leading to a ferromagnetic state of LSMO. (b) Above  $U_c$ , majority spins flow across the LSMO layer by spin-hopping process  $t$ . In contrast, the minority spins (blue arrows) will accumulate at the interface, since the spin-hopping process  $t$  is blocked by the strong interaction with the local spins due to the large Hund's rule coupling  $J_H$  (right panel). The AFM super-exchange interaction of  $t_{2g}$  electrons between neighboring Mn ions dominates, and the interfacial LSMO layer undergoes an FM-to-AFM phase transition.

See [supplementary material](#) for more information on sample preparation and characterization, optical measurements, and charge density estimation.

The MSHG experiments, data analysis, and discussions performed at the College of William and Mary were supported by the Department of Energy (Grant No. DE-FG02-04ER46127). The work at the Pennsylvania State University (PSU) was supported in part by NSF (Grant No. DMR-1411166) for sample growth and the DOE (Grant No. DE-FG02-08ER4653) for the electrical and ferroelectric characterizations.

<sup>1</sup>F. Matsukura, Y. Tokura, and H. Ohno, "Control of magnetism by electric fields," *Nat. Nanotechnol.* **10**, 209 (2015).

<sup>2</sup>R. Ramesh, "Ferroelectrics: A spin on spintronics," *Nat. Mater.* **9**, 380 (2010).

<sup>3</sup>W. Eerenstein, N. D. Mathur, and J. F. Scott, "Multiferroic and magnetoelectric materials," *Nature* **442**, 759–765 (2006).

<sup>4</sup>E. Y. Tsymlal and H. Kohlstedt, "Tunneling across a ferroelectric," *Science* **313**, 181 (2006).

<sup>5</sup>C.-G. Duan, S. S. Jaswal, and E. Y. Tsymlal, "Predicted magnetoelectric effect in Fe/BaTiO<sub>3</sub> multilayers: Ferroelectric control of magnetism," *Phys. Rev. Lett.* **97**, 047201 (2006).

<sup>6</sup>M. Gajek, M. Bibes, S. Fusil, K. Bouzouane, J. Fontcuberta, A. Barthélémy, and A. Fert, "Tunnel junctions with multiferroic barriers," *Nat. Mater.* **6**, 296 (2007).

<sup>7</sup>J. F. Scott, "Data storage: Multiferroic memories," *Nat. Mater.* **6**, 256 (2007).

<sup>8</sup>J. P. Velev, C.-G. Duan, J. D. Burton, A. Smogunov, M. K. Niranjan, E. Tosatti, S. S. Jaswal, and E. Y. Tsymlal, "Magnetic tunnel junctions with ferroelectric barriers: Prediction of four resistance states from first principles," *Nano Lett.* **9**, 427 (2009).

<sup>9</sup>V. Garcia, M. Bibes, L. Bocher, S. Valencia, F. Kronast, A. Crassous, X. Moya, S. Enouz-Vedrenne, A. Gloter, D. Imhoff, C. Deranlot, N. D. Mathur, S. Fusil, K. Bouzouane, and A. Barthélémy, "Ferroelectric control of spin polarization," *Science* **327**, 1106 (2010).

<sup>10</sup>M. Hambe, A. Petraru, N. A. Pertsev, P. Munroe, V. Nagarajan, and H. Kohlstedt, "Crossing an interface: Ferroelectric control of tunnel currents in magnetic complex oxide heterostructures," *Adv. Funct. Mater.* **20**, 2436 (2010).

<sup>11</sup>Y. W. Yin, M. Raju, W. J. Hu, X. J. Weng, X. G. Li, and Q. Li, "Coexistence of tunneling magnetoresistance and electroresistance at room temperature in La<sub>0.7</sub>Sr<sub>0.3</sub>MnO<sub>3</sub>/(Ba,Sr)TiO<sub>3</sub>/La<sub>0.7</sub>Sr<sub>0.3</sub>MnO<sub>3</sub> multiferroic tunnel junctions," *J. Appl. Phys.* **109**, 07D915 (2011).

<sup>12</sup>D. Pantel, S. Goetze, D. Hesse, and M. Alexe, "Reversible electrical switching of spin polarization in multiferroic tunnel junctions," *Nat. Mater.* **11**, 289–293 (2012).

<sup>13</sup>Y. W. Yin, M. Raju, W. J. Hu, X. J. Weng, K. Zou, J. Zhu, X. G. Li, Z. D. Zhang, and Q. Li, "Multiferroic tunnel junctions," *Front. Phys.* **7**, 380–385 (2012).

<sup>14</sup>J. D. Burton and E. Y. Tsymlal, "Magnetoelectric interfaces and spin transport," *Philos. Trans. R. Soc., A* **370**, 4840 (2012).

<sup>15</sup>C. A. F. Vaz, F. J. Walker, C. H. Ahn, and S. Ismail-Beigi, "Intrinsic interfacial phenomena in manganite heterostructures," *J. Phys.: Condens. Matter* **27**, 123001 (2015).

<sup>16</sup>C. A. F. Vaz, J. Hoffman, Y. Segal, J. W. Reiner, R. D. Grober, Z. Zhang, C. H. Ahn, and F. J. Walker, "Origin of the magnetoelectric coupling effect in Pb(Zr<sub>0.2</sub>Ti<sub>0.8</sub>)O<sub>3</sub>/La<sub>0.8</sub>Sr<sub>0.2</sub>MnO<sub>3</sub> multiferroic heterostructures," *Phys. Rev. Lett.* **104**, 127202 (2010).

<sup>17</sup>X. Ma, A. Kumar, S. Dussan, H. Zhai, F. Fang, H. B. Zhao, J. F. Scott, R. S. Katiyar, and G. Lüpke, "Charge control of antiferromagnetism at PbZr<sub>0.52</sub>Ti<sub>0.48</sub>O<sub>3</sub>/La<sub>0.67</sub>Sr<sub>0.33</sub>MnO<sub>3</sub> interface," *Appl. Phys. Lett.* **104**, 132905 (2014).

<sup>18</sup>H. Zheng, J. Wang, S. E. Lofland, Z. Ma, L. Mohaddes-Ardabili, T. Zhao, L. Salamanca-Riba, S. R. Shinde, S. B. Ogale, F. Bai, D. Viehland, Y. Jia, D. G. Schlom, M. Wuttig, A. Roytburd, and R. Ramesh, "Multiferroic BaTiO<sub>3</sub>-CoFe<sub>2</sub>O<sub>4</sub> nanostructures," *Science* **303**, 661 (2004).

<sup>19</sup>Y. W. Yin, J. D. Burton, Y.-M. Kim, A. Y. Borisevich, S. J. Pennycook, S. M. Yang, T. W. Noh, A. Gruverman, X. G. Li, E. Y. Tsymlal, and Q. Li,

- “Enhanced tunnelling electroresistance effect due to a ferroelectrically induced phase transition at a magnetic complex oxide interface,” *Nat. Mater.* **12**, 397 (2013).
- <sup>20</sup>D. Yi, J. Liu, S. Okamoto, S. Jagannatha, Y.-C. Chen, P. Yu, Y.-H. Chu, E. Arenholz, and R. Ramesh, “Tuning the competition between ferromagnetism and antiferromagnetism in a half-doped manganite through magnetoelectric coupling,” *Phys. Rev. Lett.* **111**, 127601 (2013).
- <sup>21</sup>G. Y. Yang, G. D. Lian, E. C. Dickey, C. A. Randall, D. E. Barber, P. Pinceloup, M. A. Henderson, R. A. Hill, J. J. Beeson, and D. J. Skamser, “Oxygen nonstoichiometry and dielectric evolution of BaTiO<sub>3</sub>, Part II—insulation resistance degradation under applied dc bias,” *J. Appl. Phys.* **96**, 7500 (2004).
- <sup>22</sup>H. Yamada, Y. Ogawa, Y. Ishii, H. Sato, M. Kawasaki, H. Akoh, and Y. Tokura, “Engineered interface of magnetic oxides,” *Science* **305**, 646 (2004).
- <sup>23</sup>Y. Fan, K. J. Smith, G. Lüpke, A. T. Hanbicki, R. Goswami, C. H. Li, H. B. Zhao, and B. T. Jonker, “Exchange bias of the interface spin system at the Fe/MgO interface,” *Nat. Nanotechnol.* **8**, 438 (2013).
- <sup>24</sup>D. P. Cann, J. P. Maria, and C. A. Randall, “Relationship between wetting and electrical contact properties of pure metals and alloys on semiconducting barium titanate ceramics,” *J. Mater. Sci.* **36**, 4969 (2001).
- <sup>25</sup>D. W. Reagor, S. Y. Lee, Y. Li, and Q. X. Jia, “Work function of the mixed-valent manganese perovskites,” *J. Appl. Phys.* **95**, 7971 (2004).
- <sup>26</sup>M. Bowen, M. Bibes, A. Barthélémy, J.-P. Contour, A. Anane, Y. Lemaître, and A. Fert, “Nearly total spin polarization in La<sub>2/3</sub>Sr<sub>1/3</sub>MnO<sub>3</sub> from tunneling experiments,” *Appl. Phys. Lett.* **82**, 233 (2003).
- <sup>27</sup>K. G. Rana, T. Yajima, S. Parui, A. F. Kemper, T. P. Devereaux, Y. Hikita, H. Y. Hwang, and T. Banerjee, “Hot electron transport in a strongly correlated transition metal oxide,” *Sci. Rep.* **3**, 1274 (2013).
- <sup>28</sup>M. Cinchetti, M. Sánchez Albaneda, D. Hoffmann, T. Roth, J.-P. Wüstenberg, M. Krauß, O. Andreyev, H. C. Schneider, M. Bauer, and M. Aeschlimann, “Spin-flip processes and ultrafast magnetization dynamics in Co: Unifying the microscopic and macroscopic view of femtosecond magnetism,” *Phys. Rev. Lett.* **97**, 177201 (2006).
- <sup>29</sup>P. Fazekas, *Lecture Notes on Electron Correlation and Magnetism* (World Scientific, 1999), p. 231.